scientific reports

Check for updates

OPEN

Co-evolution model of traffic travel and disease transmission under limited resources

Zhanhao Liang[1], Kadyrkulova Kyial Kudayberdievna[1], Guijun wu[1], Zhantu Liang[2]✉, Batyrkanov Jenish Isakunovich[1], Wei Xiong[1], Wei Meng[1] & Yukai Li[3]

The co-evolution mechanisms between traffic mobility and disease transmission under resource constraints remain poorly understood. This study proposes a two-layer transportation network model integrating the Susceptible-Infectious-Susceptible (SIS) epidemic framework to address this gap. The model incorporates critical factors such as total medical resources, inter-network infection delays, travel willingness, and network topology. Through simulations, we demonstrate that increasing medical resources significantly reduces infection scale during outbreaks, while prolonging inter-network delays slows transmission rates but extends epidemic persistence. Complex network topologies amplify the impact of travel behavior on disease spread, and multi-factor interventions (e.g., combined resource allocation and delay extension) outperform single-factor controls in suppressing transmission. Furthermore, reducing network connectivity (lower average degree) proves effective in mitigating outbreaks, especially under low travel willingness. These findings highlight the necessity of coordinated policies that leverage resource optimization, travel regulation, and network simplification to manage epidemics. This work provides actionable insights for policymakers to design efficient epidemic control strategies in transportation-dependent societies.

Keywords Disease transmission model, Co-evolution mechanism, Limited resources, Inter-network delay, Multi-factor control

The propagation of infectious diseases has long been a critical challenge to global public health systems, with historical pandemics underscoring their capacity to disrupt societal and economic stability[1]. The COVID-19 pandemic, emerging in late 2019, epitomized this threat through its unprecedented transmissibility and pathogenicity, inflicting profound humanitarian and infrastructural losses worldwide[2]. This crisis has intensified scholarly focus on the complex interdependencies between disease transmission dynamics and human behavioral patterns, particularly mobility-driven interactions that govern epidemic spread[3–5].

Traditional epidemiological models, including the Susceptible-Infectious (SI), Susceptible-Infectious-Susceptible (SIS), and Susceptible-Infectious-Removed (SIR) frameworks, have provided foundational insights into transmission mechanisms[6,7]. The SI model, for instance, characterizes diseases with irreversible infection states (e.g., HIV), while SIS and SIR incorporate recovery mechanisms, distinguishing between temporary immunity (SIS) and permanent immunity (SIR)[8–13]. Despite their utility, these models often oversimplify real-world complexities by neglecting the co-evolutionary feedback between individual mobility and infection spread. For instance, they fail to account for how travel behaviors dynamically reshape contact networks or how resource constraints modulate recovery rates—a gap that limits their predictive accuracy in urbanized, interconnected populations[14,15]. Then, recent advances in epidemiological modeling have leveraged fractional calculus, non-integer derivatives and optimal control theory to capture memory effects, heterogeneous interactions, partial immunity, adaptive intervention strategies and saturation dynamics inherent in complex biological systems[16–20]. For instance, studies such as ref[16]. employ fractional-calculus frameworks to analyze CD4 + T cell dynamics in HIV progression, while Jan et al. utilizes fractal-fractional operators with Caputo derivatives to model Rift Valley fever transmission, revealing critical thresholds for zoonotic spillover[17]. Similarly, ref[18]. integrates non-integer derivatives to explore memory-dependent dengue transmission, emphasizing the role of asymptomatic carriers and vaccination delays. Moreover, fractional calculus is employed to model Hand–Foot–Mouth Disease dynamics, revealing how partial immunity modulates outbreak resurgence—a critical insight for designing phased travel restrictions[19]. Similarly, Jan et al. incorporate variable source terms via the Galerkin method to

[1]Kyrgyz State Technical University named after I.Razzakov, Bishkek 720044, Kyrgyzstan. [2]Department of Artificial Intelligence and Data Science, Guangzhou Xinhua University, Dongguan 523133, Guangdong, China. [3]Zhejiang Provincial Energy Group Company Ltd, Hangzhou 310007, China. ✉email: liangzhantu2087@xhsysu.edu.cn

analyze HIV infection dynamics, emphasizing the role of time-dependent resource allocation in stabilizing infection rates[20]. These approaches address limitations of classical ODE-based models (e.g., SI, SIS, SIR) by incorporating temporal memory and spatially heterogeneous interactions—features critical for modeling adaptive human mobility under resource constraints[6,7,13].

Recent advances in network science have also bridged the divide between classical ODE-based models and realistic scenarios by modeling transportation systems as complex networks, where nodes represent individuals or hubs, and edges denote travel pathways[21,22]. Single-layer network studies, such as Chen et al.[21], demonstrated that topological metrics (e.g., node proximity) predict epidemic thresholds, while Song et al.[22] quantified network robustness against pathogen spread. However, such frameworks inadequately capture multi-scale interactions—e.g., cross-network delays between urban and rural regions or resource competition during outbreaks. Huang et al.[23] advanced this field by identifying influential links for targeted quarantine, and Basnarkov et al.[24]proposed a COVID-19-specific SEAIR model integrating asymptomatic carriers. Furthermore, network-augmented frameworks have extended the principles of fractional calculus and non-integer derivatives to systems with structured interactions[25–28]. For example, Ahmad et al. investigate computer virus propagation through modified SIR models, linking network topology to outbreak resilience[25], and fractional derivatives are applied to tungiasis dynamics[26], demonstrating how targeted interventions disrupt parasite-host cycles. Such methodologies align with our focus on transportation networks, where fractal-fractional operators[27]and saturation incidence terms[28] could further refine predictions of cross-regional transmission delays and resource-dependent recovery rates. Yet, these works largely overlook the temporal decoupling of inter-network transmission and the role of adaptive mobility under finite medical resources.

Thus, multi-layer network models have emerged as a pivotal advancement in epidemiology, addressing the oversimplifications of single-layer frameworks. Fan et al.[29]demonstrated that coupled multi-layer networks reduce infection ratios compared to single-layer analogs, as they better capture real-world social heterogeneity. This has spurred efforts to integrate adaptive human behaviors and dynamic network restructuring into transmission models[30]. For instance, Guo et al.[31] developed a two-layer time-varying network model, revealing that partial mapping between layers critically modulates epidemic thresholds—a finding corroborated by hybrid Markov chain and Monte Carlo simulations. Concurrently, Kan et al.[32]highlighted how spontaneous awareness behaviors in dual-network systems alter infection thresholds, emphasizing the need to model preventive measures alongside transmission dynamics. Dynamic networks further enhance realism by simulating behavior-driven connectivity changes, which directly influence pathogen spread[33]. These studies collectively underscore that static or homogeneous network assumptions inadequately represent the co-evolution of mobility and disease transmission.

Meanwhile, recent research has increasingly focused on quantifying how travel behavior governs epidemic outcomes. Harper et al.[34] established that optimal travel restrictions balance mobility and outbreak control, while Badr et al.[35] empirically linked COVID-19 transmission scales to population mobility patterns using mobile device data. Xiong et al.[36] further advanced this by modeling location-based mobility to predict infection risks, demonstrating that real-time mobility data can refine containment strategies. Notably, Mo et al.[37]introduced time-varying public transit encounter networks, showing that targeted transportation policies reduce superspreader events by 30–50%. These findings align with evidence that information diffusion—a key modulator of travel behavior—alters mobility patterns during outbreaks[38]. However, existing models often neglect the interplay between resource-limited recovery rates and inter-network transmission delays, limiting their utility in designing adaptive, multi-factor interventions.

Further, Jan et al. applies fractional derivatives to evaluate viral infection control policies, demonstrating that memory-dependent interventions (e.g., delayed travel bans) outperform static measures[39]. This resonates with our findings on inter-network infection delays and their context-dependent efficacy. Studies such as ref[40]. extend this paradigm to typhoid fever, quantifying how vaccination coverage and carrier identification reduce transmission thresholds—a principle applicable to optimizing resource-limited epidemic responses. More importantly, optimal control theory is employed to model co-evolving vector-borne diseases[41], providing methodological parallels to our co-evolutionary framework for mobility and transmission. Collectively, these works underscore the necessity of integrating adaptive control policies and fractional dynamics into networked epidemic models, particularly under resource constraints. Motivated by these, we propose a disease transmission model on a two-layer transportation network that comprehensively considers the total medical resources, inter-network infection delay, and travel willingness. Then, the specific innovations of this paper are as follows. (1) We propose an integrated co-evolution framework which uniquely captures the bidirectional feedback between disease transmission dynamics and adaptive travel choices under resource constraints—a gap in existing single-layer or static network models. (2) Unlike traditional constant recovery rates, our model introduces a time-varying recovery rate modulated by the total medical resource availability, reflecting real-world scenarios where healthcare capacity directly impacts epidemic outcomes. (3) The incorporation of asymmetric infection delays between subnetworks (e.g., delays from urban to rural networks) provides a nuanced understanding of how temporal decoupling in cross-network transmission influences both infection peaks and long-term persistence. (4) We systematically demonstrate that coordinated interventions—combining resource allocation, delay extension, and topology simplification—achieve superior epidemic suppression compared to isolated measures, offering a paradigm shift from conventional single-factor approaches. (5) By quantifying the sensitivity of infection rates to network complexity and travel willingness, our work establishes actionable thresholds for network connectivity reduction, enabling targeted strategies to balance mobility and public health during outbreaks. These innovations collectively advance the theoretical understanding of co-evolution mechanisms in epidemic dynamics and provide a scalable toolkit for designing context-specific containment policies in resource-limited settings.

Model and analysis

This paper employs the SIS model to characterize the spread of infectious diseases[6,7]. In the SIS model, individuals are categorized into two states: susceptible (S) and infected (I). Susceptible individuals have a certain probability of contracting the disease upon contact with infected individuals, transforming into infected individuals, while infected individuals have the opportunity to recover and revert to the susceptible state over time. The primary parameters in the SIS model are the infection rate β and the recovery rate μ. The infection process is identical to that in the SI model, while recovery occurs when an infected individual j transitions to a susceptible individual with a probability μ, denoted as $j_I \xrightarrow{\mu} j_S$. In line with refs[10,11], the dynamical modeling of the SIS model is formulated as

$$\begin{aligned} \frac{dS[t]}{dt} &= -\beta S(t) I(t) + \mu I(t) \\ \frac{dI[t]}{dt} &= \beta S(t) I(t) - \mu I(t) \end{aligned} \tag{1}$$

To describe the co-evolutionary mechanism between transportation mobility and disease transmission, drawing lessons from ref[31]. , we have constructed a two-layer transportation network comprising subnetwork A and subnetwork B. Disease transmission within both subnetworks adheres to the SIS model. Each subnetwork contains N nodes, where each node represents an individual capable of transitioning between the susceptible (S) and infected (I) states. The links between nodes signify travel contacts among individuals, serving as the avenues for disease transmission. An individual in the susceptible state (S) can be infected by infected individuals both within and across layers, while an individual in the infected state (I) has a certain probability of recovering to the susceptible state. We assume the existence of infection delays between layers but not within subnetworks.

Let β_1 denote the probability of an infected individual in subnetwork A transmitting the disease to its neighbors, ω_1 represent the probability of disease transmission from an infected node in subnetwork B to a node in subnetwork A, which also signifies the connection strength between the two layers of the transportation network, and μ_1 be the probability of an infected individual in subnetwork A recovering to the susceptible state. Similarly, β_2 is the probability of disease transmission from an infected individual in subnetwork B to its neighbors, ω_2 the probability of transmission from an infected node in subnetwork A to a node in subnetwork B, and μ_2 the recovery probability in subnetwork B. The probabilities of individual i in subnetwork A and subnetwork B being infected at time t are denoted by $p_{1i}(t)$ and $p_{2i}(t)$, respectively, and then based on ref[23]. , their dynamical equations can be expressed as

$$\frac{dp_{1i}(t)}{dt} = (1 - r_{1i}(t))(1 - p_{1i}(t)) - \mu_1(t) p_{1i}(t) + \sum_{j=1}^{N} d_{ij} p_{2j}\left(t - T_j^2\right)(1 - p_{1i}(t)) + n_1 f_1(t) \tag{2a}$$

$$\frac{dp_{2i}(t)}{dt} = (1 - r_{2i}(t))(1 - p_{2i}(t)) - \mu_2(t) p_{2i}(t) + \sum_{j=1}^{N} d_{ij} p_{1j}\left(t - T_j^1\right)(1 - p_{2i}(t)) + n_2 f_2(t) \tag{2b}$$

where $n_1(n_2)$ represents the influence of contact caused by travel willingness on disease transmission, $f_1(t)$ ($f_2(t)$) are Gaussian random numbers that vary with time, signifying the varying degree of contact due to individual travel over time, $T_j^1(T_j^2)$ denotes the delay in disease transmission from individual j in subnetwork A to individual i in subnetwork B, d_{ij} is the adjacency matrix linking individuals between subnetwork A and subnetwork B, with $d_{ij} = 1$ indicating a link between individual i in subnetwork A and individual j in subnetwork B, and $d_{ij} = 0$ indicating no link. $r_{1i}(t)$ and $r_{2i}(t)$ represent the probabilities that individual i remains uninfected by its neighbors in subnetwork A and subnetwork B, respectively, and are expressed as

$$r_{1i}(t) = \prod_{j=1}^{N} \left[1 - \beta_1 A_{ij} p_{1j}(t)\right] \tag{3a}$$

$$r_{2i}(t) = \prod_{j=1}^{N} \left[1 - \beta_2 B_{ij} p_{2j}(t)\right], \tag{3b}$$

where A_{ij} and B_{ij} are the adjacency matrices for subnetwork A and subnetwork B, respectively, taking a value of 1 if individual i is directly connected to individual j, and 0 otherwise.

In the first term of Eq. (2), $1 - r_{1i}(t)$ represents the probability that individual i is infected by at least one neighbor in subnetwork A, and $1 - p_{1i}(t)$ is the probability of individual i being infected. The second term denotes the probability that individual i is infected and has not recovered at time t. The third term accounts for the probability of individual i being infected by neighbors in subnetwork B, considering the delay in inter-network disease transmission. The fourth term incorporates the influence of travel willingness and travel-related contacts, describing the uncertainty introduced by such contacts in disease transmission. The final population infection rates in subnetwork A (subnetwork B) are given by

$$\rho_1(t) = \frac{1}{N} \sum_{j=1}^{N} p_{1j}(t) \left(\rho_2(t) = \frac{1}{N} \sum_{j=1}^{N} p_{2j}(t)\right. \tag{4}$$

In traditional SIS models, the recovery rate μ of infected individuals transitioning back to the susceptible state is often set as a constant. However, considering the variation in the number of infected individuals across different stages of disease spread, which in turn affects the resources available to individuals, μ is modeled as a time-varying parameter in this study. The recovery rate of infected individuals varies with changes in the population

infection rate. Assuming a total medical resource availability of M within the population, following ref[14]. , the time-varying function for the recovery rate is

$$\mu_i(t) = e^{-\frac{\rho_i(t)}{M}}, i = 1, 2 \tag{5}$$

To explore the evolutionary mechanisms of transportation willingness and disease transmission under the influence of inter-network infection delays, we assume subnetwork A to be a random network and subnetwork B to be a regular network, with average degrees k_1 and k_2, respectively. Under this assumption, Eq. (3) can be simplified to

$$r_{1i}(t) = [1 - \beta_1 p_{1j}(t)]^{k_1} \tag{6a}$$

$$r_{2i}(t) = [1 - \beta_2 p_{2j}(t)]^{k_2} \tag{6b}$$

From these, we derive $p_{1j} = \rho_1(t)$ and $p_{2j} = \rho_2(t)$. Furthermore, we assume that the disease transmission delays between the two subnetworks are identical, and the influence of travel willingness-induced contacts on disease transmission is the same, i.e., $T_j^1 = T_j^2 = T$ and $n_1 = n_2 = n$.

When the disease transmission reaches a steady state, let $\rho_A(t)$ and $\rho_B(t)$ represent the infection scales of subnetwork A and subnetwork B at the stable state, respectively. Their expressions are given by

$$d\rho_1(t) = \left\{ \begin{array}{c} [1 - \beta_1 \rho_1(t)]^{k_1}(1 - \rho_1(t)) - e^{-\frac{\rho_1(t)}{M}}\rho_1(t) \\ +\rho_2(t - T)(1 - \rho_1(t)) \end{array} \right\} dt + nf_1(t)\,dt \tag{7a}$$

$$d\rho_2(t) = \left\{ \begin{array}{c} [1 - \beta_1 \rho_2(t)]^{k_2}(1 - \rho_2(t)) - e^{-\frac{\rho_2(t)}{M}}\rho_2(t) \\ +\rho_1(t - T)(1 - \rho_2(t)) \end{array} \right\} dt + nf_2(t)\,dt \tag{7b}$$

When the impact of travel contacts between the two subnetworks is ignored, the relationship between the population infection rates can be derived as

$$\rho_2 = \frac{\rho_1 e^{-\frac{\rho_1(t)}{M}}}{1 - \rho_1} - \left[1 - (1 - \beta_1 \rho_1(t))^{k_1}\right] = A(\rho_1) \tag{8}$$

Based on Eqs. (7) and (8), we can obtain

$$e^{-A(\rho_1)/M} - \left[1 + \rho_1 - (1 - \beta_2 A(\rho_1))^{k_2}\right]\left(\frac{1}{A(\rho_1)} - 1\right) = 0 \tag{9}$$

If the total resource M is relatively small, Eq. (9) can be further simplified to

$$(1 + \rho_1)^{\frac{1}{k_2}} = 1 + \beta_2\left[1 - (1 - \beta_1 \rho_1)^{k_1}\right] \tag{10}$$

Under certain conditions of system parameters, ρ_1 possesses non-trivial solutions other than 0. According to Eq. (8), the existence of non-trivial solutions for ρ_1 also implies the existence of non-trivial solutions for ρ_2. By symmetry, we can deduce that $\rho_1 = \rho_2$. In this study, the total resource M, the inter-network infection delay T, and the average degree k_1 of the network are considered as controllable variables, while the travel willingness n is a system variable that requires primary attention. Most importantly, the qualitative results are robust and remain valid with respect to reasonable parameter variations, indicating the effectiveness and robustness of this model.

Results

We systematically investigated how the total medical resource availability M governs disease transmission dynamics in the two-layer network. Figure 1(a) illustrates a consistent inverse relationship between M and the steady-state infection rate ρ_1: as M increases from 0 to 1, ρ_1 declines sharply across all travel willingness levels ($n = 0 - 0.04$). For instance, at $n = 0.02$, ρ_1 drops from 0.92 to 0.15 when M rises from 0.01 to 1, underscoring the critical role of medical resources in suppressing outbreaks. Conversely, when M is fixed (e.g., $M = 0.5$), ρ_1 escalates monotonically with \(n\) (Fig. 1(b)), revealing that even moderate travel activity ($n > 0.01$) amplifies infections. Notably, under severe resource scarcity ($M = 0.01$), minimal travel willingness ($n = 0.005$) triggers near-total infection ($\rho_1 = 0.96$), highlighting the fragility of epidemic control systems with inadequate healthcare capacity. These results quantify two synergistic risks: (1) low M drastically elevates outbreak vulnerability regardless of mobility restrictions, and (2) unrestrained travel n exacerbates transmission even with sufficient M. This interplay emphasizes the necessity of dual-policy strategies that simultaneously bolster medical resources and regulate travel to prevent system collapse.

We further analyzed how inter-network infection delay T modulates the infection rate ρ_1, particularly under varying travel willingness n. Figure 2(a) reveals a counterintuitive trend: while ρ_1 marginally decreases by 1.2% (from 0.994 to 0.982) as T increases from 1 to 5 under high n (≥ 0.02), a significant reduction of 39.8% (from 0.874 to 0.526) occurs at low n ($n = 0.002$). This highlights that prolonging cross-network delays is most effective when travel activity is restricted. Figure 2(b) further contrasts these dynamics: at high

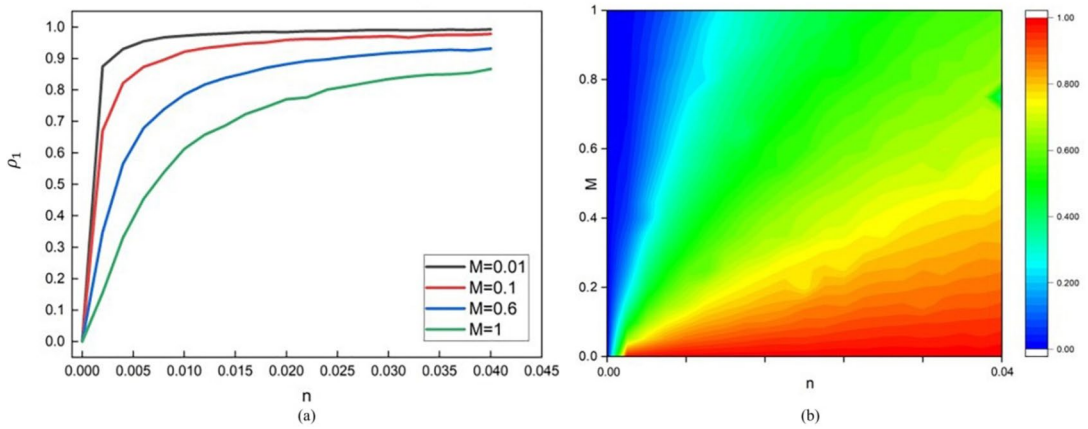

Fig. 1. Impact of total resource amount M on infection rates ρ_1. (**a**) Infection rate ρ_1 decreases monotonically with increasing total medical resources M across all travel willingness levels n. (**b**) At fixed M, ρ_1 escalates with higher n, revealing critical vulnerability under low-resource conditions ($M < 0.1$). Other parameters: Number of nodes $N = 2500$, $\beta_1 = \beta_2 = 0.05$, initial infection proportions $\rho_1(0) = \rho_2(0) = 0.01$, average degrees $k_1 = k_2 = 10$ and inter-network transmission delay $T = 1$.

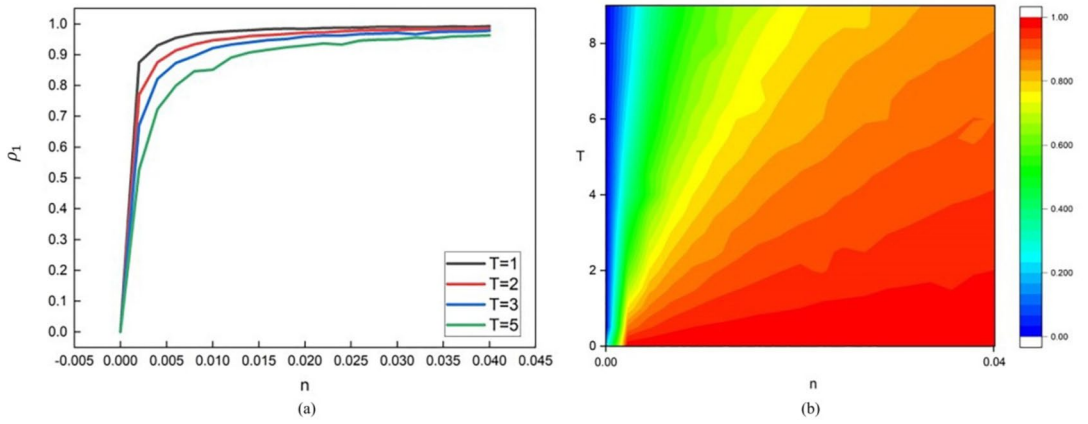

Fig. 2. Impact of inter-network infection delay T on infection rates ρ_1. (**a**) Prolonging inter-network delay T reduces ρ_1 by 39.8% at low n ($n = 0.002$) but minimally impacts high n ($n \geq 0.02$)). (**b**) Resource allocation M outperforms delay extension T in suppressing ρ_1 under high mobility ($n > 0.02$). Other parameters: Number of nodes $N = 2500$, $\beta_1 = \beta_2 = 0.05$, initial infection proportions $\rho_1(0) = \rho_2(0) = 0.01$, $k_1 = k_2 = 10$, and total resource amount $M = 0.1$..

n ($n = 0.03$), increasing T alone reduces ρ_1 by only 6%, whereas boosting medical resources M achieves a 58% reduction. This divergence underscores that delays primarily decelerate transmission chains but cannot offset the rapid spread driven by frequent travel. Practically, this implies that during high-mobility periods (e.g., holidays), policies should prioritize both delaying inter-group interactions (e.g., staggered travel schedules) and enhancing healthcare capacity to maximize containment efficacy.

Naturally, the impact of the average network degree k_1 on the disease transmission rate is also noteworthy. As shown in Fig. 3(a), while ρ_1 increases with n for all k_1, the sensitivity escalates exponentially in densely connected networks. For instance, when $k_1 = 1$, increasing n from 0 to 0.01 raises ρ_1 by 0.107, whereas for $k_1 = 10$, the same increment in n drives ρ_1 to surge by 0.85 ($\Delta\rho_1 = 0.743$). This amplification arises because higher k_1 exponentially expands contact pathways, enabling rapid transmission even under minimal travel activity. Figure 3(b) further reveals that simplifying networks ($k_1 < 4$) caps ρ_1 below 0.3 regardless of n. For example, reducing k_1 from 10 to 3 decreases peak ρ_1 by 64% under moderate travel activity $n = 0.02$), demonstrating that structural simplification (e.g., closing non-essential hubs) is a potent containment strategy.

To optimize containment, we analyzed the joint effects of medical resources M and inter-network delays T. Figure 4 shows that ρ_1 peaks in the lower-left quadrant (low M, low T) and minimizes in the upper-right quadrant (high M), high T). For instance, combining $M = 0.8$ with $T = 10$ reduces ρ_1 to 0.12, whereas isolated interventions ($M = 0.8$ alone or $T = 10$ alone) yield $\rho_1 = 0.45$ and 0.38, respectively. Beyond $T > 9.7$, ρ_1 becomes independent of M, as prolonged delays inherently decelerate transmission chains,

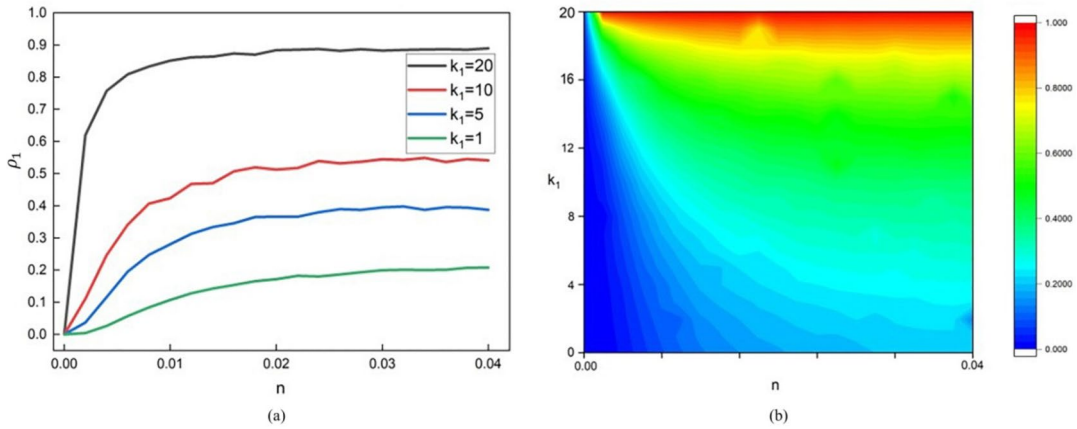

Fig. 3. Impact of average degree of subnetworks k_1 on infection rates ρ_1. (**a**) Network complexity k_1 amplifies ρ_1 sensitivity to travel willingness n, with $\Delta\rho_1 = 0.85$ for $k_1 = 10$ versus $\Delta\rho_1 = 0.1$ for $k_1 = 1$. (**b**) Simplifying networks ($k_1 < 4$) caps $\rho_1 < 0.3$ regardless of n. Other parameters: $N = 2500$, $\beta_1 = \beta_2 = 0.05$, initial infection proportions $\rho_1(0) = \rho_2(0) = 0.01$, inter-network infection delay $T = 1$, and total resource amount $M = 0.1$..

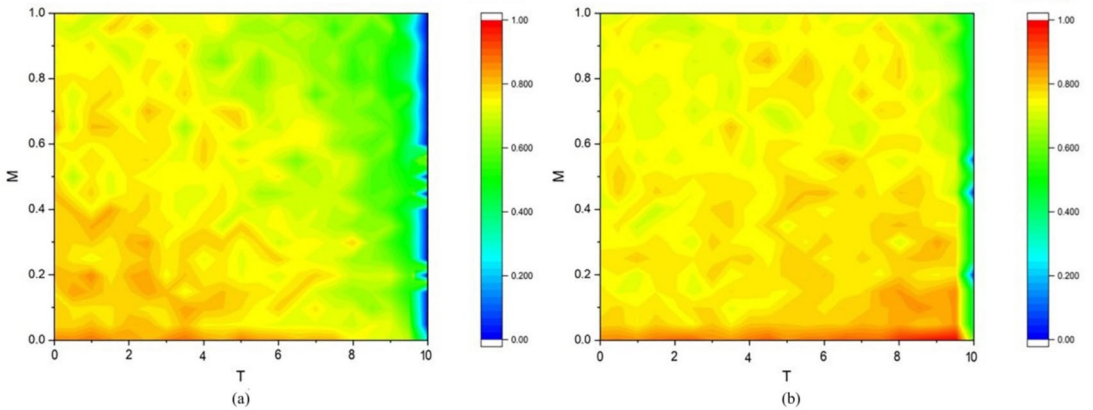

Fig. 4. Combined effect of inter-network infection delay T and total resource amount M on infection rates ρ_1. (**a**) $n = 0.004$; (**b**) $n = 0.01$. Synergistic control of T and M minimizes ρ_1 (upper-right corner: $T > 9.7$, $M > 0.8$), whereas isolated interventions fail to suppress outbreaks (lower-left corner: $T < 2$, $M < 0.2$). Other parameters: $N = 2500$, $\beta_1 = \beta_2 = 0.05$, initial infection proportions $\rho_1(0) = \rho_2(0) = 0.01$, and average degrees $k_1 = k_2 = 10$..

rendering additional resources redundant. This highlights the need for phased policies: early-stage delays (e.g., travel restrictions) paired with mid-term resource scaling.

Finally, under fixed n, we evaluated the interplay between k_1 and T. At low travel willingness ($n = 0.004$), joint modulation of k_1 and T significantly suppresses ρ_1 (e.g., $\rho_1 \approx 0.2$ for $k_1 = 3$ and $T = 8$; Fig. 5(a)). However, at high n ($n = 0.01$), structural controls lose efficacy ($\rho_1 \approx 0.4$; Fig. 5(b)), as frequent travel overrides network adjustments. This underscores that reducing n (e.g., via public awareness campaigns) is prerequisite to leveraging structural interventions. During outbreaks, policies must prioritize mobility reduction before implementing network simplification or delay extensions.

Conclusion and discussion

This study systematically investigates the co-evolutionary dynamics between traffic mobility and disease transmission under resource constraints through a two-layer transportation network model integrated with the SIS epidemic framework. The key findings are summarized as follows. (1) Increasing the total medical resource availability significantly reduces infection rates across all mobility scenarios. (2) Prolonging inter-network infection delays effectively slows transmission rates under low mobility, but becomes less impactful at high mobility. (3) Enhancing complex network topologies (increasing average degree of networks) amplify the sensitivity of infection rates to travel behavior. (4) Coordinated interventions—combining resource

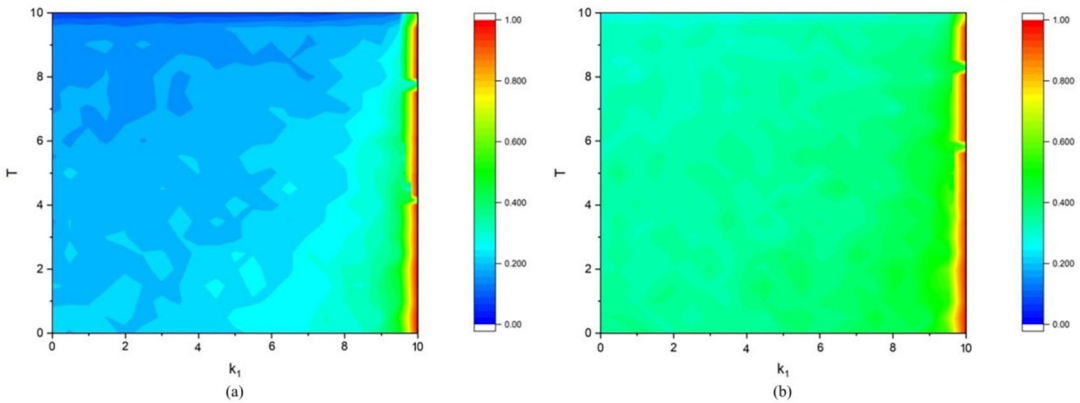

Fig. 5. Joint effect of average degree of subnetworks k_1 and inter-network infection delay T on infection rates ρ_1. (**a**) $n = 0.004$; (**b**) $n = 0.01$. At fixed n, joint modulation of k_1 and T reduces ρ_1 significantly under low mobility ($n = 0.004$, $\rho_1 \approx 0.2$) but loses efficacy under high mobility ($n = 0.01$, $\rho_1 \approx 0.4$), emphasizing mobility restriction as a prerequisite for structural controls. Other parameters: $N = 2500$, $\beta_1 = \beta_2 = 0.05$, initial infection proportions $\rho_1(0) = \rho_2(0) = 0.01$, and total resource amount $M = 0.1$..

optimization, delay extension and network simplification—achieve superior epidemic suppression compared to isolated measures.

The novelty of this work lies in its dynamic resource-dependent recovery rate, asymmetric inter-network delay mechanisms, and explicit modeling of bidirectional feedback between mobility and transmission. These advancements address gaps in traditional single-layer or static network models. Practically, the findings advocate for policies that prioritize (1) tiered resource allocation during outbreaks, (2) staggered travel schedules to maximize delays, and (3) strategic simplification of transportation networks.

Future research could extend this framework to incorporate real-time mobility data, vaccine distribution dynamics, or multi-pathogen interactions. Additionally, validating the model against empirical datasets (e.g., COVID-19 mobility patterns) would enhance its predictive power for real-world epidemic management. Overall, this study not only advances theoretical understanding of co-evolutionary epidemic systems but also provides actionable insights for policymakers to balance public health and socioeconomic mobility in resource-limited settings.

Data availability

The datasets used and/or analysed during the current study available from the corresponding author on reasonable request.

Received: 21 October 2024; Accepted: 6 March 2025
Published online: 12 March 2025

References

1. Li, K. et al. Simulated dynamics of virus spreading on social networks with various topologies. *Appl. Math. Comput.* **470**, 128580 (2024).
2. Li, Q. R. et al. Improved social force model considering the influence of COVID-19 pandemic: pedestrian evacuation under regulation. *Appl. Math. Model.* **124**, 509–517 (2023).
3. Newman, M. E. J. Spread of epidemic disease on networks. *Phys. Rev. E.* **66** (1), 016128 (2002).
4. Kandhway, K. & Kuri, J. Campaigning in heterogeneous social networks: optimal control of SI information epidemics. *IEEE/ACM Trans. Networking.* **24** (1), 383–396 (2016).
5. Wang, S. Y. & Mei, G. An efficient spreading strategy considering information decays and partial interactions between people in scale-free networks. *IEEE Access.* **7**, 95878–95891 (2019).
6. Lu, Y. L. & Liu, J. The impact of information dissemination strategies on epidemic spreading in complex networks. Physica A: Statistical Mechanics and its Applications, 536: 120920. (2019).
7. Szolnoki, A. et al. Evolution of emotions on networks leads to the evolution of Cooperation in social dilemmas. *Phys. Rev. E.* **87** (4), 042805 (2013).
8. Fu, X. et al. Epidemic dynamics on scale-free networks with piecewise linear infectivity and immunization. *Phys. Rev. E.* **77** (3), 036113 (2008).
9. Lee, H. W. et al. Social clustering in epidemic spread on coevolving networks. *Phys. Rev. E.* **99** (6), 062301 (2019).
10. Wu, Q. C. & Zhu, W. F. Toward a generalized theory of epidemic awareness in social networks. *Int. J. Mod. Phys. C.* **28** (5), 1750070 (2017).
11. Daley, D. J. & Kendall, D. G. Epidemics and rumours. *Nature* **204** (4963), 1118 (1964).
12. Pastor-Satorras, R. & Vespignani, A. Epidemic spreading in scale-free networks. *Phys. Rev. Lett.* **86** (14), 3200–3203 (2001).
13. Wang, W. et al. Coevolution spreading in complex networks. *Phys. Rep.* **820**, 1–51 (2019).
14. Zhu, P. C. et al. Analysis of epidemic spreading process in adaptive networks. *IEEE Trans. Circuits Syst. II Express Briefs.* **66** (7), 1252–1256 (2019).
15. Wang, W. et al. Asymmetrically interacting spreading dynamics on complex layered networks. **Scientific Reports**. **4**, 5097 (2014).

16. Alshammari, A. O. et al. Fractional-calculus analysis of the dynamics of CD4 + T cells and human immunodeficiency viruses. *Eur. Phys. J. Special Top.*, 1–13. (2024).
17. Jan, R. et al. Modeling rift Valley fever transmission: insights from fractal-fractional dynamics with the Caputo derivative. *Math. Modelling Control*. **4** (2), 163–177 (2024).
18. Jan, R. et al. Insights into dengue transmission modeling: index of memory, carriers, and vaccination dynamics explored via non-integer derivative. *AIMS Bioeng.*, **11**(1). (2024).
19. Jan, R. et al. Transmission dynamics of Hand–Foot–Mouth disease with partial immunity through non-integer derivative. *Int. J. Biomathematics*. **16** (06), 2250115 (2023).
20. Jan, R. & Yüzbaşı, Ş. *Dynamical Behaviour of HIV Infection With the Influence of Variable Source Term Through Galerkin Method*152111429 (Chaos, Solitons & Fractals, 2021).
21. Chen, J. et al. Optimal curing strategy for competing epidemics spreading over complex networks. *IEEE Trans. Signal. Inform. Process. Over Networks*. **7**, 294–308 (2021).
22. Song, B. et al. A novel metric to quantify the real-time robustness of complex networks with respect to epidemic models. *Front. Phys.* **9**, 790 (2022).
23. Huang, B., Yang, J. X. & Li, X. Identifying influential links to control spreading of epidemics. *Phys. A: Stat. Mech. Its Appl.* **583**, 126291 (2021).
24. Basnarkov, L. SEAIR epidemic spreading model of COVID-19. Chaos. *Solitons Fractals*. **142**, 110394 (2021).
25. Ahmad, I. et al. Dynamic behaviors of a modified computer virus model: insights into parameters and network attributes. *Alexandria Eng. J.* **103**, 266–277 (2024).
26. Shah, N. N. H. et al. Enhancing public health strategies for tungiasis: A mathematical approach with fractional derivative. *AIMS Bioeng.* **10** (4), 384–405 (2023).
27. Rehman, Z. U. et al. Computational analysis of financial system through non-integer derivative. *J. Comput. Sci.* **75**, 102204 (2024).
28. Boulaaras, S. et al. Modeling the dynamical behavior of the interaction of T-cells and human immunodeficiency virus with saturated incidence. *Commun. Theor. Phys.* **76** (3), 035001 (2024).
29. Fan, C. J. et al. Effect of individual behavior on the interplay between awareness and disease spreading in multiplex networks. *Phys. A: Stat. Mech. Its Appl.* **461**, 523–530 (2016).
30. Zhang, H. F. et al. Suppression of epidemic spreading in complex networks by local information-based behavioral responses. *Chaos: Interdisciplinary J. Nonlinear Sci.* **24** (4), 043106 (2014).
31. Guo, H. et al. Impact of information diffusion on epidemic spreading in partially mapping two-layered time-varying networks. *Nonlinear Dyn.* **105** (4), 3819–3833 (2021).
32. Kan, J. Q. & Zhang, H. F. Effects of awareness diffusion and self-initiated awareness behavior on epidemic spreading: an approach based on multiplex networks. *Commun. Nonlinear Sci. Numer. Simul.* **44**, 193–203 (2017).
33. Zhou, R. & Wu, Q. C. Epidemic spreading dynamics on complex networks with adaptive social-support. *Phys. A: Stat. Mech. Its Appl.* **525**, 778–787 (2019).
34. Harper, R. & Tee, P. Balancing capacity and epidemic spread in the global airline network. *Appl. Netw. Sci.* **6**, 94 (2021).
35. Badr, H. S. et al. Association between mobility patterns and COVID-19 transmission in the USA: A mathematical modelling study. *Lancet. Infect. Dis.* **20** (11), 1247–1254 (2020).
36. Xiong, C. F. et al. Mobile device data reveal the dynamics in a positive relationship between human mobility and COVID-19 infections. *Proc. Natl. Acad. Sci. U.S.A.* **117** (44), 27087–27089 (2020).
37. Mo, B. et al. Modeling epidemic spreading through public transit using time-varying encounter network. *Transp. Res. Part. C: Emerg. Technol.* **122**, 102893 (2021).
38. Funk, S., Gilad, E. & Jansen, V. A. A. Endemic disease, awareness, and local behavioural response. *J. Theoretical Biologys*. **264** (2), 501–509 (2010).
39. Jan, R. et al. Mathematical analysis of the transmission dynamics of viral infection with effective control policies via fractional derivative. *Nonlinear Eng.* **12** (1), 20220342 (2023).
40. Jan, R. et al. Fractional-calculus analysis of the dynamics of typhoid fever with the effect of vaccination and carriers. *Int. J. Numer. Model. Electron. Networks Devices Fields*. **37** (2), e3184 (2024).
41. Boulaaras, S. et al. Modeling the co-dynamics of vector-borne infections with the application of optimal control theory. *Discrete Continuous Dyn. Systems-S*. https://doi.org/10.3934/dcdss.2024109 (2024). (Early access).

Author contributions

Z.L. (Zhanhao Liang): Writing- Original draft preparation, Methodology, Visualization; K.K., G.W., B.J.: Software, Data curation, Investigation; W.X., Z.L.: Conceptualization, Methodology, Supervision, Writing - review & editing, Funding acquisition; W.M., Y.L.: software, Validation;

Funding

This research was supported by the Guangdong Provincial Key Discipline Research Capacity Improvement Project on 'Artificial Intelligence Application Research Based on Medical Imaging Big Data', project number: 2022ZDJS152.

Declarations

Ethics approval and consent to participate

Not applicable.

Consent for publication

Not applicable.

Competing interests

The authors declare no competing interests.

Additional information

Correspondence and requests for materials should be addressed to Z.L.

Reprints and permissions information is available at www.nature.com/reprints.